Disformal dark energy at colliders

Philippe Brax,[1,*] Clare Burrage,[2,†] and Christoph Englert[3,‡]

[1]*Institut de Physique Théorique, Université Paris-Saclay, CEA, CNRS, F-91191 Gif/Yvette Cedex, France*

[2]*School of Physics and Astronomy, University of Nottingham, Nottingham, NG7 2RD, United Kingdom*

[3]*SUPA, School of Physics and Astronomy, University of Glasgow, Glasgow, G12 8QQ, United Kingdom*

Disformally coupled, light scalar fields arise in many of the theories of dark energy and modified gravity that attempt to explain the accelerated expansion of the universe. They have proved difficult to constrain with precision tests of gravity because they do not give rise to fifth forces around static non-relativistic sources. However, because the scalar field couples derivatively to standard model matter, measurements at high energy particle colliders offer an effective way to constrain and potentially detect a disformally coupled scalar field. Here we derive new constraints on the strength of the disformal coupling from LHC run 1 data and provide a forecast for the improvement of these constraints from run 2. We additionally comment on the running of disformal and standard model couplings in this scenario under the renormalisation group flow.

I. INTRODUCTION

Evidence for the acceleration of the expansion of the universe comes from a wide variety of cosmological observations [1–4], which probe the expansion history of the universe and the way in which the distribution of light and matter has evolved to form structures. There is currently no convincing theoretical explanation for this expansion. Introduction of a cosmological constant requires an extreme fine tuning to explain why its value is so small, when quantum fluctuations of standard model fields want to drive its value to the highest energy scale of the theory [5]. In contrast to the hierarchy problem, the cosmological constant problem is a fine tuning problem that exists even at low energies (smaller than the electroweak scale) within the Standard Model. Attempts to solve the cosmological constant problem, either by introducing new fields or by modifying the gravitational sector [6, 7], typically suffer from either related fine-tuning problems or an inability to match current observations. Almost all attempts to solve the cosmological constant problem introduce new, light scalar degrees of freedom that we will call dark energy.* Therefore, even without knowing the complete explanation for the accelerated expansion of the universe, we can learn about the form of the underlying theory by studying the behaviour of the resulting dark energy scalars.

As dark energy is part of a hypothesised solution to the cosmological constant problem it is expected to interact with both standard model and gravitational fields [8]. The expectation that dark energy would couple to standard model fields has proved particularly difficult to embed in the theory, as Yukawa type interactions are excluded by the results of fifth force searches [9] to a high degree of accuracy. However these measurements only restrict one particular class of interaction between dark energy and the standard model, those that arise through a conformal coupling where matter fields move on geodesics of a metric $\tilde{g}_{\mu\nu} = A(\phi)g_{\mu\nu}$, where $g_{\mu\nu}$ is the spacetime metric and A an arbitrary function of the dark energy scalar field. A second class of interactions, termed disformal, is possible. In a disformal theory matter fields move on geodesics of the metric $\tilde{g}_{\mu\nu} = g_{\mu\nu}+B(\phi)\partial_\mu\phi\partial_\nu\phi$, where again B is an arbitrary function of ϕ. Disformal interactions have been shown to arise in the four dimensional effective theory resulting from various brane world scenarios [10, 11], in branon models [12, 13] and in theories of massive gravity [14, 15]. Disformal couplings are particularly interesting in theories where an (approximate) shift symmetry for the scalar field is used to protect the mass of the dark energy scalar, and ensure that it can remain light on cosmological scales. Unlike conformal couplings, disformal couplings to matter do not break this shift symmetry. One prime example is provided by the Goldstone modes of a global symmetry where the interaction potential results from a soft and explicit breaking of the symmetry. Axion quintessence models fall into this category and are an example of a thawing model of dark energy [16]. These theories do not make a definitive prediction for the scale of the disformal interaction, allowing it to lie anywhere between the dark energy scale $\Lambda \sim 10^{-3}$ eV and the Planck scale $M_P \sim 10^{18}$ GeV. It must therefore be determined by experiment.

In contrast to conformal couplings, which are tightly constrained by experiments, disformal couplings have proved difficult to study experimentally. In particular disformal interactions hide from fifth force searches extremely successfully because they are not sourced by static, non-relativistic matter distributions. A new approach is needed to study disformal dark energy interac-

*Electronic address: Philippe.Brax@cea.fr

†Electronic address: Clare.Burrage@nottingham.ac.uk

‡Electronic address: Christoph.Englert@glasgow.ac.uk

*We use the term dark energy to include any scalar field that is introduced as part of a solution to the cosmological constant problem, not just those that directly drive the expansion of the universe to accelerate.

tions.

Disformal interactions are derivative interactions between a light scalar field and matter, therefore they can be most efficiently probed at high energies. The possibility of using particle colliders to constrain disformally coupled scalars was first proposed by Kaloper [17]. In previous work, two of us have shown that such couplings can be studied and constrained both in terrestrial laboratories and from observations of stars [18]. A constraint was estimated from early mono-photon searches at the Large Hadron Collider (LHC) and required the coupling scale $M \gtrsim 10^2$ GeV. A comparable constraint was obtained from restricting additional energy losses in supernovae. These constraints are eleven orders of magnitude stronger than the bounds that can be obtained from local tests of gravity [19]. A variety of other observational probes of disformal couplings have been previously considered: the disformal interactions of scalars with photons can be probed in laboratory experiments [20] and astrophysical observations [21]. In models motivated by Galileon theories and massive gravity, constraints have been put on the disformal interactions from studying gravitational lensing and the velocity dispersion of galaxies [22, 23]. It has also been suggested that the fifth force mediated by a disformal Galileon scalar could explain the proton radius anomaly [24]. Further cosmological implications of disformal scalars have been considered in [25–32].

We briefly review the models considered in this paper in section II. In section III we consider constraints on this class of models that arise from precision measurements at the Large Electron Positron Collider (LEP). Specifically, we compute the oblique corrections and investigate the impact of disformally coupled scalars on the Z boson line shape. Section IV is devoted to setting constraints from LHC measurements using the full run 1 data sets available from both ATLAS and CMS. In particular we study constraints from di-lepton, mono-photon and mono-jet production in association with missing transverse energy and extrapolate promising channels to the end of run 2. We also comment on modifications to the recently discovered Higgs boson phenomenology that arise from disformally coupled scalars. Throughout we will use a "mostly minus" convention for the Minkowski metric.

II. DISFORMAL DARK ENERGY

A scalar field couples disformally to matter if matter fields move on geodesics of the metric [33]

$$\tilde{g}_{\mu\nu} = g_{\mu\nu} + B(\phi)\partial_\mu\phi\partial_\nu\phi\,, \tag{1}$$

where $g_{\mu\nu}$ is the space time metric, and B is an arbitrary function of the scalar field ϕ. In this work we will only consider $B(\phi) = 1/M^4$, where M is a constant with dimensions of mass. This is the leading order term in a Taylor expansion of $B(\phi)$ and will be sufficient to demonstrate the effects of a disformal coupling at the LHC which will appear first at order $(E/M)^2$, where E is the characteristic energy of the process under discussion. The value of ϕ may very from place to place in the universe leading to a possible redressing of the scale M, which would need to be taken into account in order to compare constraints derived from different places correctly. We will not discuss variations in the background value of ϕ further in this work.

Matter fields are conserved with respect to the metric in equation (1) so that

$$\tilde{D}_\mu \tilde{T}^{\mu\nu} = 0\,, \tag{2}$$

where $\tilde{D}_\mu$ is the covariant derivative with respect to the disformal metric of equation (1), and

$$\tilde{T}^{\mu\nu} = \frac{2}{\sqrt{-\tilde{g}}}\frac{\delta S_m}{\delta \tilde{g}_{\mu\nu}} \tag{3}$$

is the Jordan frame energy momentum tensor.

The interactions between the scalar field ϕ and standard model fields that arise from interactions with the metric in equation (1) occur at all orders in $(E/M)^4$, however if we are only interested in the leading order effects of the disformal coupling then the relevant interaction terms in the action are

$$S = \frac{1}{M^4}\int d^4x\sqrt{g}\partial_\mu\phi\partial_\nu\phi T^{\mu\nu}\,, \tag{4}$$

where now $T^{\mu\nu} = (2/\sqrt{-g})(\delta S_m/\delta g_{\mu\nu})$ is the Einstein frame energy-momentum tensor, defined with respect to the space-time metric $g_{\mu\nu}$. In this work we restrict our attention to interactions of the form given in Equation (4), other possible derivative interactions of the same mass dimension are discussed in the Appendix. However we will show in Section V that if they are initially chosen to be absent additional operators are not generated by quantum corrections at order $1/M^4$.

Equation (4) motivates two approaches to observe or constrain models with disformally coupled scalars at colliders. The first avenue is through modifications to the standard model expectation for processes at precision machines such as LEP through either direct production of the scalar, which modifies for example the Z boson phenomenology or through internal quantum corrections that lead to a deviation from the standard model (SM) expectation, for example for two to two particle scattering. The second avenue is provided by exploiting the current energy frontier of the LHC. Derivative disformal couplings induce deviations at large momentum transfers, which are directly accessible to current searches. Since the scalar ϕ is light and stable on collider scales, established dark matter searches for missing energy [34–37] also provide sensitive strategies to look for disformal couplings.

III. CONSTRAINTS FROM ELECTROWEAK PRECISION MEASUREMENTS

A. Oblique corrections

A customary way of assessing the impact of new physics on standard model processes is via its impact on precision measurements performed during the LEP era. A framework which is typically adopted to analyse modifications in the gauge sector are the oblique corrections parametrised by the S, T, U parameters of Peskin and Takeuchi [38, 39]:

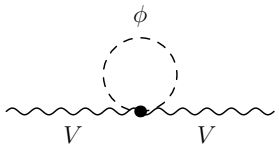

FIG. 1: One-loop and leading $1/M^4$ contribution to the vector $V = \gamma, W^\pm, Z$ polarization functions $\Pi_{\mu\nu}(q^2) = \Pi(q^2)g_{\mu\nu} + \dots$ mediated by a virtual disformal scalar coupling.

$$S = \frac{4s_w^2 c_w^2}{\alpha}\left(\frac{\Pi_{ZZ}(m_Z^2)-\Pi_{ZZ}(0)}{m_Z^2} - \frac{c_w^2-s_w^2}{c_w s_w}\frac{\Pi_{\gamma Z}(m_Z^2)-\Pi_{\gamma Z}(0)}{m_Z^2} - \frac{\Pi_{\gamma\gamma}(m_Z^2)}{m_Z^2}\right), \tag{5a}$$

$$T = \frac{1}{\alpha}\left(\frac{\Pi_{WW}(0)}{m_W^2} - \frac{\Pi_{ZZ}(0)}{m_Z^2} - \frac{2s_w}{c_w}\frac{\Pi_{\gamma Z}(0)}{m_z^2}\right), \tag{5b}$$

$$U = \frac{4s_w^2}{\alpha}\left(\frac{\Pi_{WW}(m_W^2)-\Pi_{WW}(0)}{m_W^2} - c_w^2\frac{\Pi_{ZZ}(m_Z^2)-\Pi_{ZZ}(0)}{m_Z^2} - s_w^2\frac{\Pi_{\gamma\gamma}(m_Z^2)}{m_Z^2} - 2s_w c_w\frac{\Pi_{\gamma Z}(m_Z^2)-\Pi_{\gamma Z}(0)}{m_Z^2}\right), \tag{5c}$$

where the Π functions denote SM vector boson polarization functions and c_W, s_W are cosine and sine of the weak mixing angle, respectively. From their definition it becomes obvious that the Peskin-Takeuchi parameters capture beyond the standard model (BSM)-induced effects in the gauge sector in a q^2 expansion of the polarization functions to leading order. S, T, U parametrise "universal" modifications due to BSM physics in the gauge sector, i.e. the parameters provide an approximation to the full next-to-leading order results under the assumption that the BSM physics arises in the gauge sector only. As such, consistency with existing constraints on the Peskin-Takeuchi parameters should not be understood as consistency of a particular model with electroweak precision measurements, it merely acts as a first test that a particular model has to pass.

The contributions of the disformally coupled scalar at one loop and leading order in $1/M^4$ are sketched in Fig. 1. The polarization function for the photon reads:

$$\Pi_{\gamma\gamma}(q^2) = \frac{q^2}{32\pi^2}\left(\frac{m_\phi}{M}\right)^4. \tag{6}$$

This is consistent with intact gauge invariance. For broken directions (and $Z-\gamma$ mixing) we have

$$\Pi_{\gamma Z}(q^2) = 0\,, \tag{7}$$

$$\Pi_{VV}(q^2) = \frac{1}{128\pi^2}\left(m_\phi^2(4q^2-3m_V^2) + 10m_V^2 A_0(m_\phi^2)\right)\left(\frac{m_\phi}{M^2}\right)^2, \tag{8}$$

where $V = W^\pm, Z$ and $A_0(m^2)$ is the scalar loop function in the Passarino Veltman language [41, 42] in D-dimensional regularisation

$$A_0(m^2) = \frac{(2\pi\mu)^{4-D}}{i\pi^2}\int \mathrm{d}^D q\,\frac{1}{q^2-m^2} = -m^2\left(\frac{m^2}{4\pi\mu^2}\right)^{D/2-2}\Gamma\left(1-\frac{D}{2}\right), \tag{9}$$

where μ is the so-called 't Hooft mass that keeps track of mass units in D dimensions and cancels in renormalised quantities. With these equations, it is easy to see that the contributions of the $\sim q^0, q^2$ pieces to the Peskin-Takeuchi parameters Eq. (5) vanish identically. Note that due to the appearance of only A_0 functions in the gauge boson self-energies $\sim q^2$ there are no contributions to the extended set of precision observables as defined in [43], which capture the impact of BSM effects on the vector boson self-energies $\sim q^4$. Therefore no constraints can be placed on the disformal coupling scale M from precision measurements of S, T and U. We will comment on the impact on running couplings in section V.

B. Z boson phenomenology

Another important and precisely determined quantity is the lineshape of the Z boson. Since the disformal coupling dresses every interaction vertex and the scalar mass can be significantly below the Z boson threshold a novel $1 \to 4$ channel will open at leading order in the $1/M^4$ expansion. Depending on the size of M, this can lead to a significant modification of the Z bosons decay phenomenology and the Z boson lineshape as a consequence.

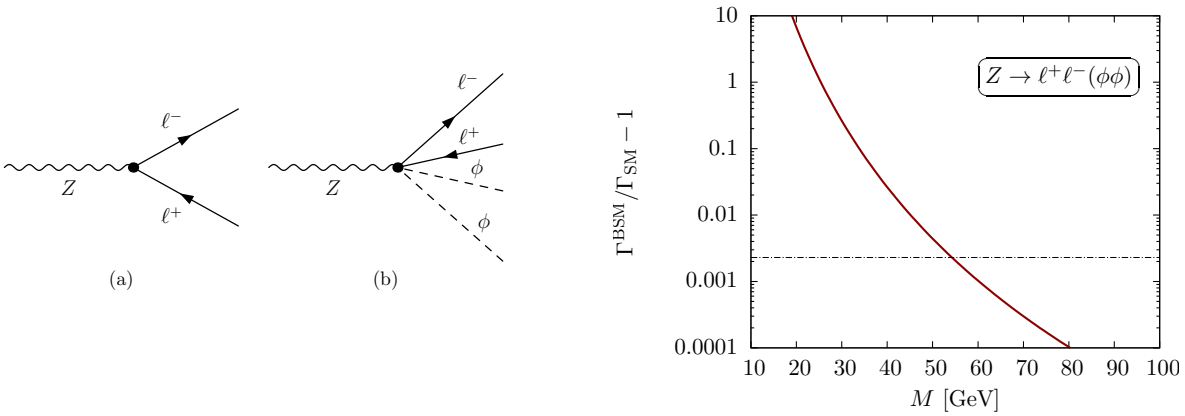

FIG. 2: Modification of the Z boson width to leptons (here concretely for $Z \to \ell^+\ell^- = \{e^+e^-, \mu^+\mu^-, \tau^+\tau^-\}$) due to "dressing" the decay using the new interaction with two scalars. The leading order Feynman diagram contributing to this decay is shown in (a) and an example diagram contributing to the modification of the decay at $\sim 1/M^4$ is shown in (b). Note that the individual fermion legs and the Z boson propagator can also be dressed with a ϕ^2 insertion and these diagrams are not shown. Similarly the production of the Z boson receives modifications. The vertical line gives the current bound on $Z \to \ell^+\ell^-$ [40].

The size of the BSM correction as a function of M is shown in Fig. 2. We can use this to set a lower limit on M; however an explicit calculation shows that this lower bound is only weak, $M \gtrsim 60$ GeV.

Given that $Z \to \ell^+\ell^-\phi\phi$ is a four body decay, it is worthwhile to compare this decay mode to another four body decay mode, $Z \to \ell^+\ell^-\ell^+\ell^-$ in the SM. The above constraint, $M \gtrsim 60$ GeV, on the new interactions arises from saturation the error on the 2 lepton decay which is 0.23%. The four lepton branching ratio, however, is 4.6×10^{-6} [40]. Calculating the branching ratio $Z \to \ell^+\ell^-\phi\phi$ for $M \simeq 60$ GeV we find the branching to disformal scalars to be 15 times bigger than the $Z \to \ell^+\ell^-\ell^+\ell^-$ in the SM.

IV. CONSTRAINTS FROM LHC SEARCHES

The form of the disformal coupling means that disformal scalars can be produced on shell in a collider and, as they will not interact in the detector, will leave only missing energy as a signature of their presence. This means that missing energy searches for dark matter can be adapted to place constraints on disformally coupled dark energy models. In this section we recast recent analyses performed by ATLAS and CMS in the monojet [34], mono-photon [35, 36] and di-lepton [37] searches, where available, to reinterpret these measurements and set constraints on the scale M.[†] By validating our analysis against the 8 TeV results we can also extrapolate our findings to the upcoming run 2 and estimate the limit that will be set in the near future.

For the actual analyses we include the signal and all dominant backgrounds and simulate them with FeynRules [46], MadEvent [47], Sherpa [48] and Herwig++ [49], jet clustering is performed with FastJet [50]. Our analysis is independent of the mass of the scalar field as, in all models, this mass is expected to be much smaller than the momentum transfer of the processes under consideration.

Setting limits on effective field theories at colliders can suffer from shortcomings if the new physics scale is resolved by the experiment [51–56]. An effective field theory description is only valid if the probed energy scales are lower than the scale of new physics, e.g. if resonances or thresholds remain unresolved. These shortcomings can be mended by reverting to concrete UV complete scenarios (but limits become model dependent as a consequence) or by separating energy scales consistently on the basis of renormalisation group equations [51, 57]. In the scenario we consider in this paper it is important to highlight a difference compared to similar issues in dark matter searches: while complete field theoretic models can be constructed in dark matter-related analyses, a concrete model implementation is not available in the analysis of strongly coupled gravitational effects due to the intrinsic non-linear and non-renormalisable nature of gravity in a perturbative field theory context. In what follows, this issue should be kept in mind; while limit setting is a viable qualitative strategy in the absence of a signal, the interpretation of a possible excess seen with M in the TeV region will require the inclusion of non-linear effects which are formally higher order in our $(E/M)^4$ expansion. We will comment on the validity of the set limits in light of resolved energy scales later in section V.

[†]Mono-lepton searches [44, 45] crucially depend on a correct modeling of the missing energy resolution, and we do not consider these searches.

Mono-Photon searches

Both ATLAS and CMS have published analyses in mono-photon searches for the full run 1 data set [35, 36] with similar sensitivities. We can use these measurements to constrain disformal scalars at the LHC via the $pp \to \phi\phi\,\gamma$ production, where the ϕ escapes undetected, hence leading to a mono-photon signature.

CMS reconstruct jets using the anti-k_T algorithm [58] to cluster particles into jets with resolution parameter[‡] $D = 0.5$ and define isolated photons based on the energy deposit in a cone of $\Delta R = \sqrt{\Delta\Phi^2 + \Delta\eta^2} < 0.3$ (where Φ and η are the azimuthal angle and pseudo-rapidity, respectively) around the photon candidate, which is required to be smaller than 5% of the candidate's energy based on the expected shower profile. The transverse energy of the photon is required to be $E_T(\gamma) > 145$ GeV. Since a full detector simulation is not available, we approximate this energy with the Monte Carlo information for the transverse momentum. Events with more than one jet with $p_T > 30$ GeV and light leptons (isolation is based on a hadronic energy deposit in the vicinity of $\Delta R < 0.3$ by less than 20% of the candidate p_T) with $p_T > 10$ GeV are vetoed if they are separated from the photon by $\Delta R > 0.5$. The final selection requires a missing transverse energy $E_T^{\rm miss} > 140$ GeV, well separated from the photon in azimuthal angle $\Delta\Phi(E_T^{\rm miss}, \gamma) > 2$. We include an expected missing energy resolution by fitting the expectation of CMS particle flow as outlined in [60]. After these steps CMS exclude an upper cross section limit of 14 fb. We reproduce this cross section for a choice of $M = 419$ GeV. Therefore the CMS measurement results in a lower limit of

$$\text{CMS:} \quad M \gtrsim 419 \text{ GeV}\,. \tag{10}$$

ATLAS follow a similar strategy, selecting photons with $p_T(\gamma) > 125$ GeV in $|\eta_\gamma| < 1.37$, $E_T^{\rm miss} > 150$ GeV and $\Delta\Phi(E_T^{\rm miss}, \gamma) > 0.4$. Jets are reconstructed with the anti-k_T algorithm with $D = 0.4$ and vetoed if $p_{T,j} > 30$ GeV and $\Delta\Phi(E_T^{\rm miss}, j) < 0.4$. Electrons ($p_T > 7$ GeV, $|\eta| < 2.47$) and muons ($p_T > 6$ GeV, $|\eta| < 2.5$) are vetoed. ATLAS exclude 6.1 fb at 95% confidence level for the run 1 luminosity of 20.3/fb. Similar to interpreting this measurement in terms of a disformal scalar production in association with a hard photon, $pp \to \phi\phi\,\gamma$, this translates in our implementation into

$$\text{ATLAS:} \quad M \gtrsim 447 \text{ GeV}\,, \tag{11}$$

which is consistent with the CMS limit.

[‡]For readers less familiar with jet physics the D parameter refers to the conical size of the jet combined from particle tracks in the azimuthal angle–pseudo-rapidity plane. An excellent review of jet physics is provided in [59].

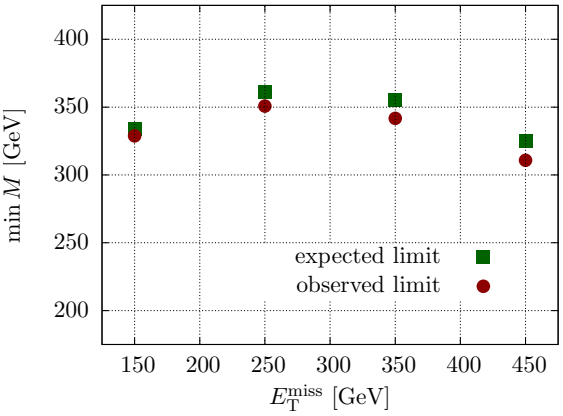

FIG. 3: Results of the ATLAS dilepton search confronted with disformal scalar coupling model. For further details see the text. ATLAS do not quote uncertainties and hence we only show central values. The relevant observed (expected) exclusion cross sections are 2.7 fb (3 fb), 0.57 fb (0.73 fb), 0.27 fb (0.36 fb), and 0.26 fb (0.27 fb) for the shown bins in missing transverse energy.

Di-Lepton searches

ATLAS have published a dark matter search in a Z+missing energy search based on the run 1 data set in [37]. We can confront this analysis with $pp \to \phi\phi\,Z$ where $Z \to$ leptons in the disformal scalar model. In their analysis, ATLAS require electrons to have $E_T > 20$ GeV, $|\eta| < 2.47$ and consider muons with $p_T > 20$ GeV, $|\eta| < 2.5$. Isolation is defined by requiring the hadronic energy deposit in a cone of size $\Delta R < 0.2$ around the candidate to be less than 10% of the candidate's E_T and only tracks with $p_T > 1$ GeV are considered in this isolation criterion. Jets are reconstructed with the anti-k_T algorithm with $D = 0.4$, and $p_T > 25$ GeV and $|\eta| < 2.5$.

Candidate events need to have a di-lepton system consistent with the Z boson 76 GeV $\leq m_{\ell\ell} \leq$ 106 GeV and the missing energy has to be well separated from the di-lepton pair: $\Delta\Phi(E_T^{\rm miss}, \ell\ell) > 2.5$. Further, ATLAS impose $\eta^{\ell\ell} < 2.5$, $|p_T^{\ell\ell} - E_T^{\rm miss}|/p_T^{\ell\ell} < 0.5$. Events with jets with $p_T > 25$ GeV are finally removed and ATLAS consider four search regions based on a inclusive selection of missing energy and provide expected and observed fiducial cross sections at 95% confidence level.

Implementing these analysis steps, we can again translate these limits into lower limits on the disformal coupling scale M, as depicted in Fig. 3. The sensitivity is maximised for the $E_T^{\rm miss} > 250$ GeV search region, where the trade off between differential signal cross section enhancement due to the probed energy in the disformal coupling and decreasing background cross sections becomes optimal. For more stringent requirements, the signal becomes kinematically suppressed.

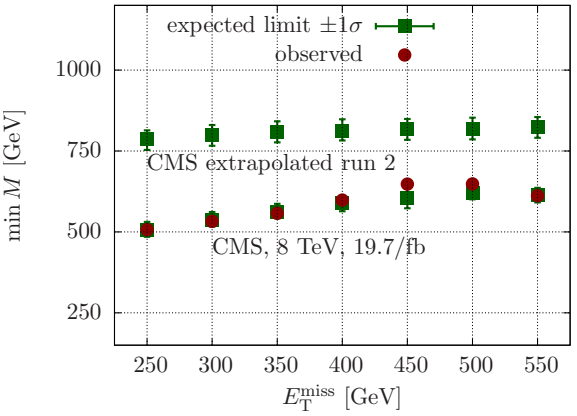

FIG. 4: Minimum scale M extracted from the CMS mono-jet search of [34] in the different search regions based on the inclusive search regions characterised by $E_T^{\rm miss}$ (for details see text). The observed excluded cross sections are 211 fb, 98.4 fb, 48.8 fb, 20.2 fb, 7.82 fb, 6.09 fb, and 7.21 fb for the shown bins in increasing order of missing transverse energy. We also show the improvement based on an extrapolation of the 8 TeV analysis to the 13 TeV LHC run 2 with 100/fb. We estimate the expected excluded cross sections for this luminosity to be 1.58 fb, 1.04 fb, 0.72 fb, 0.54 fb, 0.41 fb, 0.31 fb and 0.25 fb.

Mono-Jet searches

The most recent mono-jet analysis exploiting the full run 1 data set has been provided by the CMS collaboration in [34]. We can confront this analysis with $pp \to \phi\phi + \text{jet}$ in the disformal scalar model. In this analysis particles are clustered into jets using the anti-k_T algorithm [58] with $D = 0.5$ and requiring the leading jet to have transverse momentum and rapidity

$$p_{T,j_1} > 110 \text{ GeV}, |\eta_{j_1}| < 2.4\,. \tag{12}$$

A second jet

$$p_{T,j_2} > 30 \text{ GeV}, |\eta_{j_2}| < 4.5 \tag{13}$$

is allowed if it is separated from the first jet by

$$\Delta\Phi(j_1, j_2) < 2.5\,. \tag{14}$$

The analysis vetos events with more than two jets with $p_T > 30$ GeV and $|\eta_j| < 4.5$. Events with isolated leptons are vetoed if $p_{T,\ell} > 10$ GeV; isolation is defined by requiring the total hadronic energy deposit in a cone of size 0.4 around the lepton candidate being smaller than 20% of its transverse momentum. The analysis selects 7 inclusive search regions based on an additional missing energy threshold.

We validate our analysis in these different search regions, taking into account the Z+jets, QCD-jets, $t\bar{t}$+jets, W + jets and diboson+jets backgrounds and missing energy resolution is included in an analogous manner to that of the previous sections. We find excellent agreement of our analysis with the CMS background templates, especially for the dominant backgrounds and most inclusive selections. The agreement of our simulation with the Z + jets template in particular, provides confidence that we can set a trustable limit on the presence of an additional missing energy contribution that is the main signature of our model in this channel. For the fake-dominated background contributions as QCD jets, we use the CMS results to derive a differential efficiency, which we will later use in our 13 TeV projections without further modification.

The results of the 8 TeV CMS analysis, recast along the above lines is shown in Fig. 4. Comparing the findings of the mono-jet search to the previously discussed channels, we see that the mono-jet search is the most sensitive to our scenario. In light of this result we extrapolate the 8 TeV CMS to LHC run 2 in Fig. 4 using the CLs method of [61, 62]. Most of this improvement stems from a significant signal cross section increase by a factor of 10. It is not entirely unexpected that this particular analysis performs better than the other channels discussed above. The particular form of the interaction basically amounts to QCD-like BSM production suppressed by the scale M, and the relative sensitivity follows the paradigm that events induced by strong couplings give tighter constraints on new physics than those produced by weak couplings because jet production is the most abundant high transverse momentum process at the LHC.

A note on modified Higgs phenomenology

Finally we comment on potential modification of Higgs phenomenology. The crucial observable is the "signal strength"

$$\mu_{ik} = \frac{[\sigma_{\{i\}}(H) \times \text{BR}(H \to \{k\})]^{\rm BSM}}{[\sigma_{\{i\}}(H) \times \text{BR}(H \to \{k\})]^{\rm SM}}\,, \tag{15}$$

this measures the cross sections for Higgs production via mechanism i and subsequent decay into final state k with decay probability $\text{BR}(h \to \{k\})$, relative to the SM expectation of the same production and decay. Measurements of the Higgs signal strength have already reached considerable sensitivity $\sim 10\%$ around the SM hypothesis, but are mostly driven by the gluon fusion production mechanism. It is expected that we can scrutinize the Higgs boson's phenomenology at the percent level at the high luminosity LHC [63, 64]. "Dressing" the Higgs vertices with the additional interactions analogous to the Z boson phenomenology (see Fig. 2) at LEP, we can understand the allowed error as a limit on the scale M with the benefit of a higher mass scale $m_h > m_Z$. The modifications of the signal strength for the different decay modes are shown in Fig. 5. Whilst Higgs phenomenology is sensitive to the presence of a disformal scalar, direct searches for missing energy remain a more powerful probe.

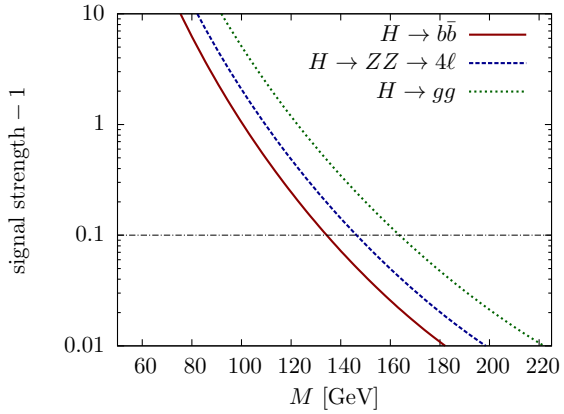

FIG. 5: Modifications of the Higgs boson signal strength as a function of M for the gluon fusion production mode at 8 TeV, estimated using Higgs effective field theory [65–67]. The modifications are analogous to the 2-body and 4-body decay sample Feynman diagrams shown in Fig. 2.

V. RUNNING OF COUPLINGS

In the previous sections we have focused on direct measurements of and constraints on the presence of a disformal interaction. In section III A we saw that the disformal scalar does not lead to oblique corrections. Not all BSM effects are expressed through oblique corrections and we analyse other observables in the following. We will see that these effects are highly suppressed and limited to kinematic thresholds in the limit $m_\phi/M \ll 1$, where we can trust our expansion in terms of an effective field theory deformation of the SM. We will also comment on potential modifications of the running of couplings due to the presence of the disformal interactions.

Taking the contribution to the vector polarization functions as a starting point we can check whether the presence of the additional derivatively-coupled scalars impacts the running of SM couplings. In particular any impact on the top Yukawa couplings, as well as on the Higgs self interaction will have important consequences on the stability of the electroweak vacuum. By working out the $\sim M^{-4}$ corrections to wave function renormalisations and SM vertices we can compute potential contributions to the SM β functions. Introducing the $\overline{\text{MS}}$ parameter in $D = 4 - 2\varepsilon$ dimensional regularisation

$$\Delta = \frac{\Gamma(1+\varepsilon)}{\varepsilon}\left(\frac{4\pi\mu^2}{\mu_R^2}\right)^{\varepsilon} \tag{16}$$

we have $A_0(m^2) = m^2\Delta + \mathcal{O}(\varepsilon)$. μ_R is the renormalisation scale that effectively replaces μ in the renormalisation procedure. We can calculate the renormalisation $\sim 1/M^4$ of the Higgs and top wave functions in the $\overline{\text{MS}}$ scheme (note that all corrections vanish in the limit $m_\phi \to 0$ in dimensional regularisation)

$$\delta Z_H = \frac{1}{32\pi^2}\,\Delta\left(\frac{m_\phi}{M}\right)^4, \tag{17}$$

$$\delta Z_t = \frac{3}{64\pi^2}\,\Delta\left(\frac{m_\phi}{M}\right)^4. \tag{18}$$

The renormalisation of the $\bar{t}tH$ vertex to $\sim 1/M^4$ is

$$\delta Z_{\bar{t}tH} = \frac{1}{16\pi^2}\,\Delta\left(\frac{m_\phi}{M}\right)^4, \tag{19}$$

which leads to an operator renormalisation

$$\delta Z = \delta Z_{\bar{t}tH} - \delta Z_t - \frac{1}{2}\delta Z_H = 0\,, \tag{20}$$

which implies no contribution $\sim 1/M^4$ to the anomalous dimension of the Yukawa coupling y_t and its running is therefore not affected by the presence of the disformal coupling.

Similarly we can compute the renormalisation of the quartic interaction operator in the Higgs potential by investigating the four point vertex H^4 (Fig. 6)

$$\delta Z_{H^4} = \frac{3}{8\pi^2}\,\Delta\left(\frac{m_\phi}{M}\right)^4 \tag{21}$$

and again we find an operator renormalisation

$$\delta Z = \delta Z_{H^4} - 2\,\delta Z_H = 0\,, \tag{22}$$

meaning that again the disformal scalar has no impact on the running of the quartic Higgs interaction.

We have checked that similar cancellations happen in the renormalisation of all other SM couplings. This cancellation is not an accident, but happens due to the independence of the external and internal symmetries of the considered effective field theory.

The deformation of the disformal interactions, on the other hand, has a dynamic dependence on scale which, if external and internal symmetries are independent, should be limited to the interaction itself as well as invariants of the external (diffeomorphisim) symmetry. Due to the complicated dynamics of the SM as a whole, to analyse this we focus on a simple subsector of the SM; QED with the top as a single massive fermion. Concretely we look at the renormalisation of the operator

$$\mathcal{O}_{\text{dis}} = \frac{c_T}{M^4}T^{\mu\nu}\partial_\mu\phi\partial_\nu\phi \tag{23}$$

and specifically at the dressed top propagator as probe of the Wilson coefficient c_T.

In this model, the wave function renormalisation for the scalar ϕ is given by

$$\delta Z_\phi = \frac{21}{8\pi^2}\,\Delta\left(\frac{m_t}{M}\right)^4 \tag{24}$$

and the full top renormalisation, including the $1/M^0$ part in general gauge is

$$\delta Z_t = \frac{\alpha}{9\pi}\,\Delta\,\xi + \frac{3}{64\pi^2}\,\Delta\left(\frac{m_\phi}{M}\right)^4, \tag{25}$$

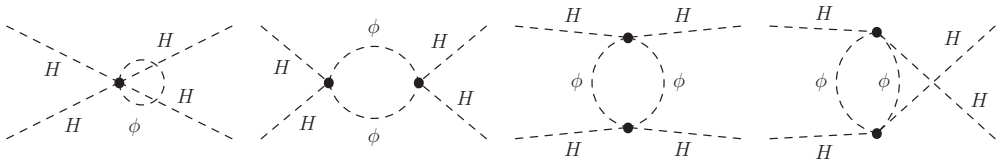

FIG. 6: One-loop corrections to the H^4 operator at order $1/M^4$.

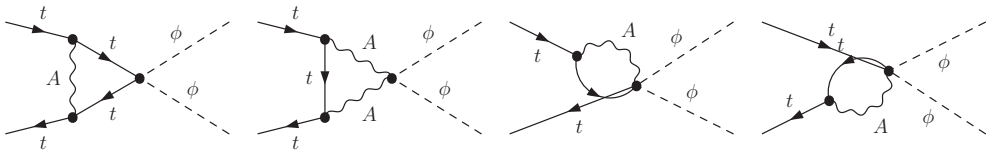

FIG. 7: One-loop corrections to the $t\bar{t}\phi\phi$ vertex in the considered toy model, extended by the disformal coupling.

where ξ is the gauge parameter. The ϕ^2-dressed top propagator, Fig. 7 is renormalised by

$$\delta Z_{t\bar{t}\phi^2} = \frac{\alpha}{9\pi}\,\Delta\,\xi \tag{26}$$

and therefore the operator renormalisation constant is (see e.g. [68] for a detailed discussion of renormalisation in effective field theories)

$$\delta Z_{\mathcal{O}_{\rm dis}} = -\frac{3}{64\pi^2}\,\Delta\,\left(\frac{m_\phi}{M}\right)^4 - \frac{21}{8\pi^2}\,\Delta\,\left(\frac{m_t}{M}\right)^4\,, \tag{27}$$

which implies an anomalous dimension

$$\gamma_{c_T} \;=\; \frac{\mathrm{d}\,\delta Z_{\mathcal{O}_{\rm dis}}}{\mathrm{d}\log\mu_R} \;=\; \frac{1}{16\pi^2}\left[\frac{3}{2}\left(\frac{m_\phi}{M}\right)^4 + 84\left(\frac{m_t}{M}\right)^4\right], \tag{28}$$

such that the renormalisation group equation (RGE) reads

$$c_T(\Lambda) = \left(\frac{\Lambda}{M}\right)^{\gamma_{c_T}} \qquad (\Lambda \leq M) \tag{29}$$

after inserting the boundary condition $c_T(M) = 1$. Since the anomalous dimension is positive definite, it flows to small coupling in the infrared, consistent with the behavior of a coupling that parametrises the interaction with SM energy-momentum. It is important to note that when calculating the operator renormalisation in Eq. (27) we do not obtain spurious singularities, which would need to be absorbed by additional counter terms unrelated to $\mathcal{O}_{\rm dis}$. The presence of such terms would be tantamount to a RGE flow-induced mixing of $\mathcal{O}_{\rm dis}$ with other independent operators[§] that are excluded from our effective theory of Eq. (23) at the UV scale (by construction). While such terms could in principle be present, see the appendix, our constraints can be understood as consistent limits on the operator $\mathcal{O}_{\rm dis}$ alone.

Furthermore, in the previous sections we have found limits in the 650 GeV range, which are mass scales easily resolved by the LHC at 8 TeV. In principle this raises the question of whether we can trust our effective field theory prescription if the most sensitive region to the presence of disformal couplings is given by $p_{T,j} > M$ in, e.g., the mono-jet analysis. However, equipped with the above RGE equations we can separate the scale of measurement and new physics consistently (see e.g. [51] for a related discussion in Higgs phenomenology): If the new physics scale is indeed higher than the resolved scale we can compute the modified limit using RGE equations like Eq. (29). Since the top quark is the heaviest particle in the SM, we can expect that Eq. (29) also gives a reasonable estimate of the size of these effects in the full SM. If we push the fundamental scale M outside the LHC coverage the effectively resolved scale due to Eq. (29) remains numerically unchanged due to the smallness of the anomalous dimension γ_{c_T} and our limit is solid against these aforementioned issues.

The findings for the running of the disformal coupling deserve a few additional remarks. Firstly, the renormalisation is not only gauge-invariant, i.e. the terms $\sim \xi$ drop out, but all terms $\sim 1/M^0$ cancel in the calculation. This means that the internal symmetries which are expressed as the zeroth order in the $\sim M^{-4}$ expansion do not influence the running of the disformal coupling. The leading term in the renormalisation only depends on invariants of Lorentz symmetry (masses and gauge couplings) and arises purely from wave function renormalisation constants (Eq. (26) is pure gauge), meaning that the coupling remains universal under renormalisation group flow. This is an explicit realisation of the result derived in [69] by Hui and Nicolis, who demonstrated that once a universal coupling between a scalar field and matter has

[§]Independent in this context means that redundancies are removed with equations of motion.

been postulated, this coupling is stable against classical and quantum renormalisations in the matter sector.

If we take the calculation at face value (and neglect the potential presence of higher order terms) the running of c_T (with UV boundary condition $c_T(M) = 1$) is given as a function of all masses in the theory, which displays the running of the energy momentum tensor by all explicit sources of the breaking of conformal invariance.¶ The running is not influenced by the gauge couplings, this demonstrates that the dynamics of internal and external symmetries factorize reminiscent of the general structure discussed by Coleman and Mandula [71].

VI. CONCLUSIONS

If dark energy couples to matter disformally our best chances to detect these interactions come from events occurring at high energies: While precision measurements at LEP provide a bound on M, the LHC offers the best current prospects for such a study, and we have shown that mono-jet searches performed by the CMS collaboration provide the best current constraint on the energy scale of the disformal coupling $M \gtrsim 650$ GeV. This bound should only be applied to disformal scalars with canonical kinetic terms. The kinetic structure of disformally coupled Galileons will modify the behaviour of the scalar at high energies, and therefore the analysis we present here does not apply. In particular, this means that our new bound on the strengh of the disformal coupling does not apply to the Galileon model used to explain the proton radius anomaly.

The particular form of the interactions, coupling to the energy momentum tensor, decouples the disformal scalar from precision electroweak observables as well as from the running of SM couplings, in agreement with the expectation of a factorisation of outer and inner symmetries in interacting QFT. This leaves direct detection as the main collider avenue to set constraints on the presence of disformal couplings. To this end we extrapolate the CMS mono-jet result to the higher energy collisions at the 13 TeV LHC run 2 and estimate that the 8 TeV result can be improved to $M \gtrsim 750$ GeV for a run 2 luminosity of 100 fb^{-1}, or even higher if systematics are improved.

Acknowledgments

We would like to thank Nemanja Kaloper and David Seery for very helpful discussions during the preparation of this work. PhB acknowledges partial support from the European Union FP7 ITN INVISIBLES (Marie Curie Actions, PITN- GA-2011- 289442) and from the Agence Nationale de la Recherche under contract ANR 2010 BLANC 0413 01. CB is supported by a Royal Society University Research Fellowship. CE is supported in part by the IPPP Associateship programme and is grateful to the Mainz Institute for Theoretical Physics (MITP) for its hospitality and its partial support during the completion of this work.

Appendix: Additional interactions

In this work we have studied the leading order behaviour when matter fields move on geodesics of a purely disformal metric. However if we wanted to relax this assumption there are a two other possible types of operator that would allow the scalar field to interact with matter in a universal way that have the same mass dimension as those considered here. Firstly, the scalar field may also couple conformally to matter. If this coupling is purely a function of the scalar derivatives then the leading order interaction with matter is:

$$(\beta/M^4)(\partial\phi)^2 T \tag{A.1}$$

for constant β. Secondly, additional terms arise because the energy momentum tensor of the matter fields is only uniquely defined up to addition of terms proportional to the equations of motion. In general relativity the energy momentum tensor remains finite under the renormalisation group flow after allowing for the inclusion of such terms [72]. For the Higgs scalar in Minkowski space, for example, this allows for the inclusion the term

$$R(\tilde{g})|H|^2 \tag{A.2}$$

where $\tilde{g}_{\mu\nu}$ is the disformal metric of Eq. (1), and R is the associated Ricci scalar. Written explicitly in terms of the disformal scalar this allows for the inclusion of interactions of the form

$$\frac{\gamma}{M^4}((\Box\phi)^2 - \nabla_\mu\nabla_\nu\phi\nabla^\mu\nabla^\nu\phi)|H|^2 \tag{A.3}$$

We stress, however, that if β and γ are assumed initially to be zero, as in the main body of this article, then they remain zero under the renormalisation group flow, at least to order $(E/M)^4$. If these terms are allowed to be non-zero then the renormalisation group is expected to mix these coefficients with c_T via the equations of motion.

[1] G. Efstathiou, W. Sutherland, and S. Maddox, Nature **348**, 705 (1990).
[2] S. Perlmutter et al. (Supernova Cosmology Project), Astrophys.J. **517**, 565 (1999), astro-ph/9812133.
[3] A. G. Riess et al. (Supernova Search Team), Astron.J. **116**, 1009 (1998), astro-ph/9805201.

[4] O. Lahav and A. R. Liddle (2014), 1401.1389.
[5] S. Weinberg, Rev.Mod.Phys. **61**, 1 (1989).
[6] E. J. Copeland, M. Sami, and S. Tsujikawa, Int.J.Mod.Phys. **D15**, 1753 (2006), hep-th/0603057.
[7] T. Clifton, P. G. Ferreira, A. Padilla, and C. Skordis, Phys.Rept. **513**, 1 (2012), 1106.2476.
[8] A. Joyce, B. Jain, J. Khoury, and M. Trodden, Phys.Rept. **568**, 1 (2015), 1407.0059.
[9] E. Adelberger, B. R. Heckel, and A. Nelson, Ann.Rev.Nucl.Part.Sci. **53**, 77 (2003), hep-ph/0307284.
[10] C. de Rham and A. J. Tolley, JCAP **1005**, 015 (2010), 1003.5917.
[11] T. Koivisto, D. Wills, and I. Zavala, JCAP **1406**, 036 (2014), 1312.2597.
[12] J. Alcaraz, J. Cembranos, A. Dobado, and A. L. Maroto, Phys.Rev. **D67**, 075010 (2003), hep-ph/0212269.
[13] J. Cembranos, A. Dobado, and A. L. Maroto, Phys.Rev. **D70**, 096001 (2004), hep-ph/0405286.
[14] C. de Rham, G. Gabadadze, and A. J. Tolley, Phys.Rev.Lett. **106**, 231101 (2011), 1011.1232.
[15] C. de Rham and G. Gabadadze, Phys.Rev. **D82**, 044020 (2010), 1007.0443.
[16] J. A. Frieman, C. T. Hill, A. Stebbins, and I. Waga, Phys.Rev.Lett. **75**, 2077 (1995), astro-ph/9505060.
[17] N. Kaloper, Phys.Lett. **B583**, 1 (2004), hep-ph/0312002.
[18] P. Brax and C. Burrage, Phys.Rev. **D90**, 104009 (2014), 1407.1861.
[19] J. Sakstein, JCAP **1412**, 012 (2014), 1409.1734.
[20] P. Brax, C. Burrage, and A.-C. Davis, JCAP **1210**, 016 (2012), 1206.1809.
[21] P. Brax, P. Brun, and D. Wouters (2015), 1505.01020.
[22] M. Wyman, Phys.Rev.Lett. **106**, 201102 (2011), 1101.1295.
[23] S. Sjors and E. Mortsell, JHEP **1302**, 080 (2013), 1111.5961.
[24] P. Brax and C. Burrage, Phys. Rev. **D91**, 043515 (2015), 1407.2376.
[25] M. Zumalacarregui, T. Koivisto, D. Mota, and P. Ruiz-Lapuente, JCAP **1005**, 038 (2010), 1004.2684.
[26] T. S. Koivisto, D. F. Mota, and M. Zumalacarregui, Phys.Rev.Lett. **109**, 241102 (2012), 1205.3167.
[27] D. Bettoni, V. Pettorino, S. Liberati, and C. Baccigalupi, JCAP **1207**, 027 (2012), 1203.5735.
[28] C. van de Bruck, J. Morrice, and S. Vu, Phys.Rev.Lett. **111**, 161302 (2013), 1303.1773.
[29] P. Brax, C. Burrage, A.-C. Davis, and G. Gubitosi, JCAP **1311**, 001 (2013), 1306.4168.
[30] J. Neveu, V. Ruhlmann-Kleider, P. Astier, M. Besanon, A. Conley, et al., Astron.Astrophys. **569**, A90 (2014), 1403.0854.
[31] C. van de Bruck and J. Morrice (2015), 1501.03073.
[32] P. Brax, C. Burrage, A.-C. Davis, and G. Gubitosi, JCAP **1503**, 028 (2015), 1411.7621.
[33] J. D. Bekenstein, Phys.Rev. **D48**, 3641 (1993), gr-qc/9211017.
[34] V. Khachatryan et al. (CMS) (2014), 1408.3583.
[35] V. Khachatryan et al. (CMS) (2014), 1410.8812.
[36] G. Aad et al. (ATLAS), Phys.Rev. **D91**, 012008 (2015), 1411.1559.
[37] G. Aad et al. (ATLAS), Phys.Rev. **D90**, 012004 (2014), 1404.0051.
[38] M. E. Peskin and T. Takeuchi, Phys.Rev. **D46**, 381 (1992).
[39] M. E. Peskin and T. Takeuchi, Phys.Rev.Lett. **65**, 964 (1990).
[40] K. Olive et al. (Particle Data Group), Chin.Phys. **C38**, 090001 (2014).
[41] G. Passarino and M. Veltman, Nucl.Phys. **B160**, 151 (1979).
[42] A. Denner, Fortsch.Phys. **41**, 307 (1993), 0709.1075.
[43] R. Barbieri, A. Pomarol, R. Rattazzi, and A. Strumia, Nucl.Phys. **B703**, 127 (2004), hep-ph/0405040.
[44] V. Khachatryan et al. (CMS) (2014), 1408.2745.
[45] G. Aad et al. (ATLAS), Phys.Rev. **D90**, 012004 (2014), 1404.0051.
[46] A. Alloul, N. D. Christensen, C. Degrande, C. Duhr, and B. Fuks, Comput.Phys.Commun. **185**, 2250 (2014), 1310.1921.
[47] J. Alwall, M. Herquet, F. Maltoni, O. Mattelaer, and T. Stelzer, JHEP **1106**, 128 (2011), 1106.0522.
[48] T. Gleisberg, S. Hoeche, F. Krauss, M. Schonherr, S. Schumann, et al., JHEP **0902**, 007 (2009), 0811.4622.
[49] M. Bahr, S. Gieseke, M. Gigg, D. Grellscheid, K. Hamilton, et al., Eur.Phys.J. **C58**, 639 (2008), 0803.0883.
[50] M. Cacciari, G. P. Salam, and G. Soyez, Eur.Phys.J. **C72**, 1896 (2012), 1111.6097.
[51] C. Englert and M. Spannowsky, Phys.Lett. **B740**, 8 (2015), 1408.5147.
[52] O. Buchmueller, M. J. Dolan, and C. McCabe, JHEP **1401**, 025 (2014), 1308.6799.
[53] P. Harris, V. V. Khoze, M. Spannowsky, and C. Williams, Phys.Rev. **D91**, 055009 (2015), 1411.0535.
[54] T. Jacques and K. Nordstrm (2015), 1502.05721.
[55] M. R. Buckley, D. Feld, and D. Goncalves, Phys.Rev. **D91**, 015017 (2015), 1410.6497.
[56] U. Haisch and E. Re (2015), 1503.00691.
[57] G. Isidori, A. V. Manohar, and M. Trott, Phys.Lett. **B728**, 131 (2014), 1305.0663.
[58] M. Cacciari, G. P. Salam, and G. Soyez, JHEP **0804**, 063 (2008), 0802.1189.
[59] G. P. Salam, Eur.Phys.J. **C67**, 637 (2010), 0906.1833.
[60] C. Englert, M. Spannowsky, and C. Wymant, Phys.Lett. **B718**, 538 (2012), 1209.0494.
[61] A. L. Read, J.Phys. **G28**, 2693 (2002).
[62] A. L. Read, CERN-OPEN-2000-205 (2000).
[63] C. Englert, A. Freitas, M. Mhlleitner, T. Plehn, M. Rauch, et al., J.Phys. **G41**, 113001 (2014), 1403.7191.
[64] M. Klute, R. Lafaye, T. Plehn, M. Rauch, and D. Zerwas, Europhys.Lett. **101**, 51001 (2013), 1301.1322.
[65] B. A. Kniehl and M. Spira, Z.Phys. **C69**, 77 (1995), hep-ph/9505225.
[66] J. R. Ellis, M. K. Gaillard, and D. V. Nanopoulos, Nucl.Phys. **B106**, 292 (1976).
[67] M. A. Shifman, A. Vainshtein, M. Voloshin, and V. I. Zakharov, Sov.J.Nucl.Phys. **30**, 711 (1979).
[68] G. Buchalla, A. J. Buras, and M. E. Lautenbacher, Rev.Mod.Phys. **68**, 1125 (1996), hep-ph/9512380.
[69] L. Hui and A. Nicolis, Phys.Rev.Lett. **105**, 231101 (2010), 1009.2520.
[70] C. Englert, J. Jaeckel, V. Khoze, and M. Spannowsky, JHEP **1304**, 060 (2013), 1301.4224.
[71] S. R. Coleman and J. Mandula, Phys.Rev. **159**, 1251 (1967).
[72] L. Brown, *Quantum field theory* (1992).